Wireless Measurement of Temperature Using Surface Acoustic Waves Sensors

L. Reindl[1], I. Shrena[1], S. Kenshil[1], R. Peter[2]
[1]Institute of Electrical Information Technology, Clausthal University of Technology, Clausthal-Zellerfeld, Germany
[2]Baumer Electric AG, Frauenfeld, Switzerland

Abstract—**Surface acoustic wave devices can be used as wireless sensor elements (SAW transponders) for measuring physical quantities such as temperature that do not need any power supply and may be accessed wirelessly. A complete wireless sensor system consists of such a SAW transponder and a local radar transceiver, is widely discussed. The antenna of the SAW transponder receives an RF burst in the VHF/UHF band transmitted by the radar transceiver. The reader unit performs a radar measurement of the impulse response of the SAW transponder via a high-frequency electromagnetic radio link. A temperature variation changes the SAW velocity and thereby the response pattern of the SAW device. By analyzing the time delay between backscattered pulses with different time delays we get a coarse estimation of the temperature of the SAW transponder. By using this information the ambiguity of ±2π in the phase differences between the pulses can be eliminated, which provides to an overall temperature resolution of ±0.2°C.**

***Key words*- Temperature sensor, passive sensors, surface acoustic waves, transponder, and radio waves.**

I. INTRODUCTION

Using surface acoustic waves (SAW) devices, a wireless readout of the temperature of a passive sensor can be achieved. The sensors are passive devices and are absolute maintenance free, light and reliable. The lifetime of such a sensor is not limited to the lifetime of the lifetime of a battery.

SAW devices are special micro acoustic components consisting of a piezoelectric substrate with metallic structures such as interdigital transducers (IDTs) and reflection or coupling gratings deposited on its plain-polished surface. Due to the piezoelectric effect an RF input signal will stimulate a micro acoustic wave propagating on the surface of the substrate. SAW technology has been exploited for electronic analogue signal processing over the past 30 years, with the development of a tremendous amount of devices and systems for consumer, commercial and military applications running now at some billion dollar annual rate.

Many piezoelectric single crystal substrates, like $LiNbO_3$ or $LiTaO_3$ show a non-vanishing temperature coefficient of delay. Hereby, a temperature variation strains the SAW chip and also changes the SAW velocity by influencing the elastic constants of the crystal substrate. Thus, by carefully analyzing the impulse response of a given SAW device on these materials, it is possible determine the temperature of the SAW chip. By using a SAW identification (ID) tag [2], [3] this SAW based sensor technique can be implemented with sensor elements such as transponders that do not need any power supply and which are connected to their reader unit solely by a wireless radio link [4]-[6]. The passive transponder responses with an RF signal - like a radar echo - which can be received by the front-end of the local transceiver. The amplitude and phase of this RF response signal carry information on the distance L of the reflectors relative to the IDT and the SAW velocity V_{SAW}. Fig. 1 shows a SEM photo of two SAW pulses, which were emitted by an IDT. Vice versa, a SAW wave generates an electrical charge distribution at the receiving IDT and therefore an electrical RF output signal occurs [1].

Fig. 2 shows the operating principle of such a sensor system. A local radar transceiver (TRx) used as reader unit sends out a radio frequency (RF) electromagnetic read-out signal in the VHF/UHF band. This read-out signal is picked up by the antenna of the passive SAW transponder and conducted to an interdigital transducer (IDT). The IDT converts the received signal into a SAW signal by the converse piezoelectric effect. The SAW propagates towards several reflectors distributed in a characteristic pattern. A small part of the wave is reflected at each reflector. The micro acoustic wave packets now returning to the IDT are re-converted into electrical signals by the IDT and re-transmitted to the radar TRx unit by the transponder antenna as illustrated in Fig. 3.

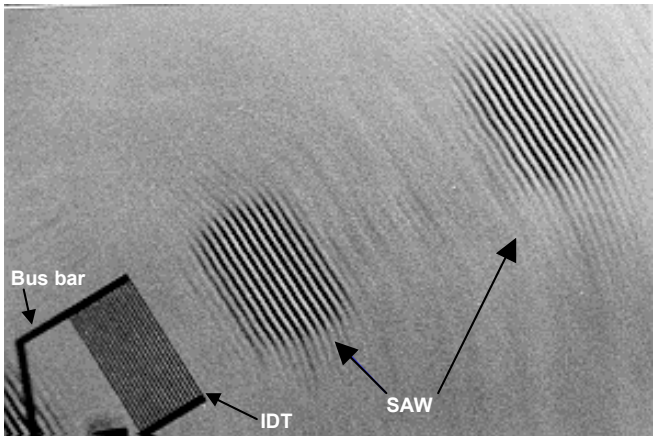

Fig. 1. SEM-photo of an interdigital transducer and two SAW pulses. (Photo by Siemens AG)

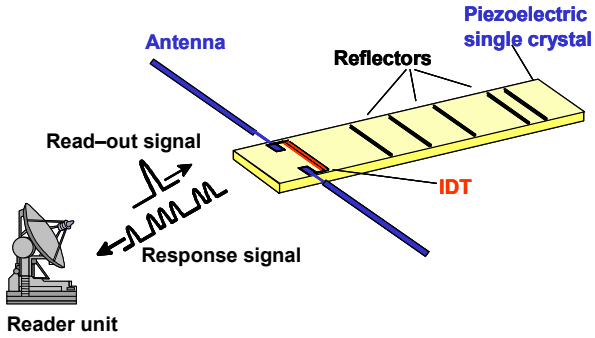

Fig. 2. Schematic of the operating principle of a SAW-based radio-link temperature measurement system.

The temperature affects the velocity of the micro acoustic wave V_{SAW} and thereby also the time distances of the RF transponder response. The evaluation of this response signal in the radar unit thus allows the determination of the environmental temperature of the passive SAW transponder.

Since such sensors need neither wiring nor batteries they can be placed advantageously on moving or rotating parts and in hazardous environments such as contaminated areas or high voltage plants, chemical or vacuum process chambers, under concrete, etc. On the other hand, SAW transponders cannot be addressed individually. Using time division techniques typically 5 to 10 different SAW sensors, each with 3-4 reflectors, could be build up.

This paper will show a detailed description and analysis of a high precision wireless measurement system for temperature using surface acoustic waves (SAW) sensors. Section II describes the local radar TRx and its specifications. The SAW transponder and its specification are investigated in section III. The measurement set up is explained in section IV. In section V the measurement results and the evaluation of the temperature are discussed. A conclusion with remarks on the accuracy of such a system will close the paper.

II. Reader Unit

The read out units of wireless SAW sensor systems resemble those used in traditional radar systems [7]. In Europe, only two frequency bands suitable for SAW devices are allocated to unlicensed low power devices (LPDs) such as industrial, scientific, or medical (ISM) apparatus: 433.0-434.77 MHz and 2.4-2.483 GHz. The allowed equivalent isotropically radiated power (EIRP) in these bands is $P_0 = 10$ mW.

For the investigation presented here, we used a commercial reader unit for SAW ID tags from Baumer Ident (see Fig. 4). The centre frequency of the used bandwidth can be chosen between 2422 MHz up to 2450 MHz. The sweep bandwidth B is 40 MHz, which gives spacing between adjacent samples $\Delta\tau_{FFT}$ of 25 ns. The system uses a frequency modulated continuous wave (FMCW) principle with a sweep time of 16 ms. Thus, the applied beat frequency is given by 2,5 Hz/ns. The radiated output power (EIRP) can be chosen between 0.01 and 10 mW according standards FCC part 15 / I-ETS 300440. The system obtains a read out distance of up to 6 m depending on the tag attenuation loss and the reader antenna. Two serial interfaces (RS 232 and RS 422) allow data transmission to an external PC or host system. In its normal mode the reader gives out the ID number of every tag, which passes the beam of the reader antenna. The reader, however, can also be operated in a service mode, in which it delivers the sampled real base band data of each measurement cycle. Applying a Fourier transformation to this data and scaling the result with the beat frequency of the FMCW system gives the impulse response of the received signal.

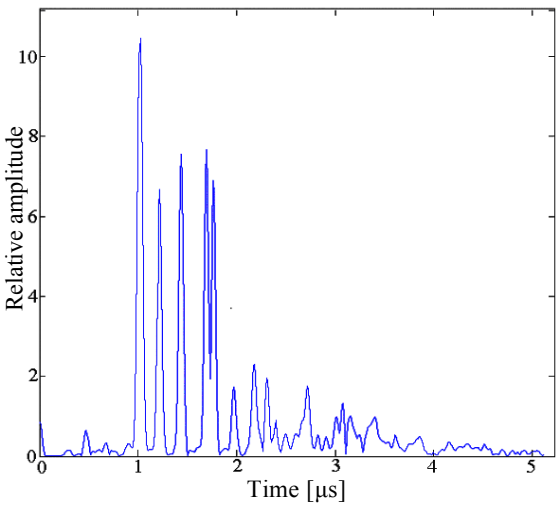

Fig.3. Time domain impulse response of the investigated SAW tag with five reflectors.

Fig 4. 2.45 GHz SAW reader unit by Baumer Ident.

III. SAW Transponder

For wireless SAW transponders we used commercial ID-tags from Baumer Ident. They use a pulse positioning coding scheme with five reflectors. Fig. 5 shows the working principle of such a pulse position coded SAW tag. The local position of each individual reflector and thus the time position of the corresponding reflected signal could be chosen out of several slots. The tag we used utilizes 10 allowed slots for each reflector, which gives a code range of 10^4 with four code reflectors and one calibration reflector. Similar types are currently developed which offer a code range of 20 to 64 bits [8]. The initial delay between the IDT and the first reflector is 1.2µs, the coding time slots are 25 ns spaced. Fig. 6 shows the mounted SAW chip in a SMD package. The Material of the piezoelectric single crystal is black Lithium niobat, $LiNbO_3$; the propagation direction is rot-128°. The corresponding propagation velocity V_{SAW} of the SAW is 3960 m/s at room temperature, which gives for 2.45 GHz a wavelength λ of 0.8µm.

The electrode material is Aluminum (Al). The bi-directional IDT is placed near the centre of the chip with three reflectors to the left and two to the right. The two bright lines parallel to the acoustic path are bus bars for the electrical wiring of the IDT to the pins of the SMD package. The package is hermetically sealed to protect the surface of the chip and then connected to an antenna to finish the SAW transponder.

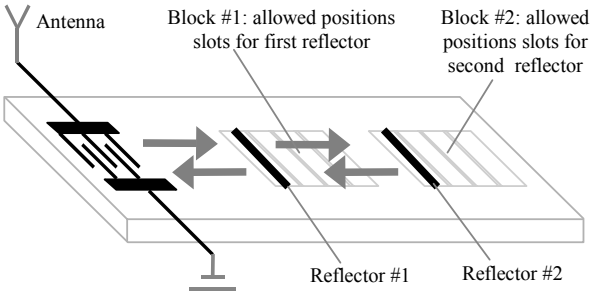

Fig. 5. Pulse position coding scheme for SAW tags.

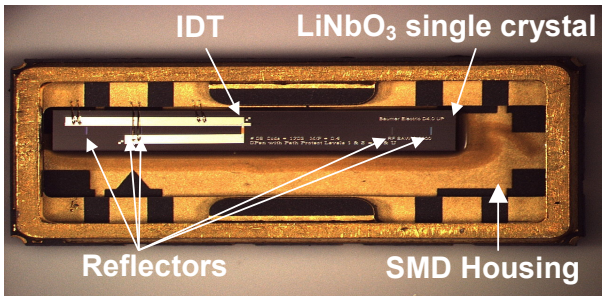

Fig. 6. Photo of an assembled SAW tag by Baumer Ident.

IV. Measurement Set up

A. Temperature Measurement and Control

Fig. 7 shows the used set up for the wireless temperature measurement. For the temperature measurements we connected the Baumer reader unit to a RF antenna. The SAW tag was placed in the beam of the antenna inside of a temperature controlled oven. The electromagnetic waves linked between the RF antenna and the SAW tag antenna through a small glass window. For temperature control an additional NiCr-Ni-thermocouple in good thermal contact to the SAW tag was used. The reader unit was connected to a computer for a detailed signal analysis using the RS 232 interface. Thereby the computer program could read out the sampled real base band data of each read out cycle and could also control all settings of the reader unit.

B. Signal Analysis

For signal analysis the numerical MATLAB tool was used. The interface to the reader unit was established by the use of the MEX file option of MATLAB, which allows the call of external developed C routines [10]. Fig. 3 illustrates the impulse response of the investigated SAW tag where the first and largest response starts at 1.2 µs. Then there are two well-separated impulses followed by two interfering signals. Finally we get several smaller spurious signals due to multi-path reflections between the coding structures and reflections by the chip edge.

C. Reader Set up

In the first step we optimised the frequency range of the reader system to ensure a perfect base band adjustment of the mixed down Rx signals of the SAW tag. This is performed if the transfer function of the antenna and the SAW reflective delay line is symmetrically to the centre of the frequency band of the *Tx* read out signal. In this case the mixed down SAW signal will be arranged symmetrically to zero frequency. By evaluating the mixed down impulse response in a polar diagram, the frequency adjustment can

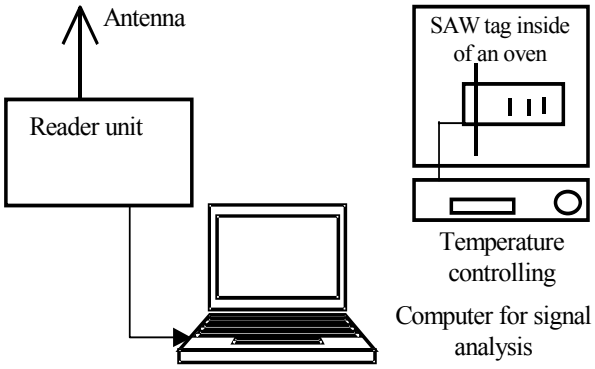

Fig. 7. Used set up for the wireless temperature measurement.

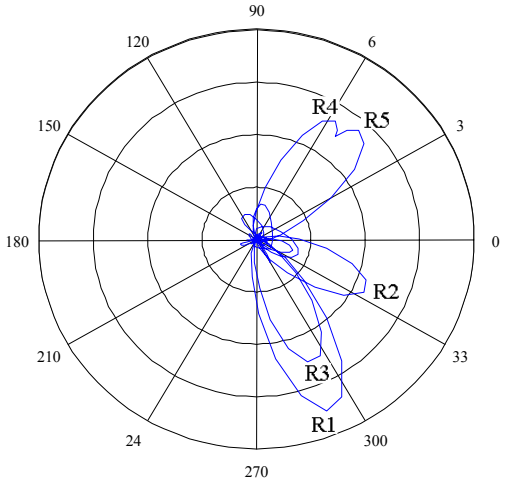

Fig. 8. Polar map of the SAW response signal in the base band measured with a FMCW signal centred at 2430 MHz

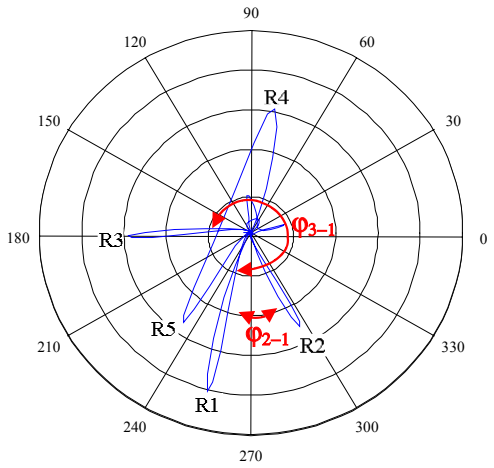

Fig. 9. Polar map of the SAW response signal in the base band measured with a FMCW signal centred at 2422 MHz

most easily be done. Any shift in frequency with respect to zero frequency will result in a phase modulation within the peaks, which broadens the spikes. Fig. 8 and 9 show the obtained time domain data by using a read-out frequency range starting with 2.410 GHz and 2.402 GHz, respectively, which corresponds to a centre frequency of f_0=2.430 GHz and f_0=2.422 GHz. For all further investigations this latter frequency range was used, because this setting resulted in the smallest spikes. There remained, however, an inter-symbol interference between the signals from reflector 4 and 5.

V. Measurement Results

Fig. 10 gives a flow chart of the used data analysis. The sampled 512 real base band data of each measurement cycle of the Baumer reader unit were read out via the RS-232 interface and transferred to Matlab using the MEX file. The ambient temperature of the SAW tag was noted and controlled as well. For improving the signal to noise ratio an averaging over several reading cycles could be performed.

Previous to the Fourier transformation we applied a weighting function to the data to minimize the spurious level in time domain. Due to its excellent side lobe level performance we used a Blackman-Harris weighting function, but this led to a huge pulse spreading of w=1.9 if compared to the unweighted one. Maybe the intersymbol interference between the signals from reflector 4 and 5 could have been avoided by using a weighting function with a smaller spreading function, e.g. a Hamming window. To improve the resolution we applied a zero padding scheme with additional 512 points before performing the Fourier transformation. The resulting spacing of the point's $\Delta\tau_{FFT}$ after the Fourier transformation becomes:

$$\Delta\tau_{FFT} = \frac{1}{2 \cdot B},$$

To calculate the exact time position of each impulse we constructed a parable approximation through the local maximum of the amplitude #1 and both adjacent points #2 and #3 as illustrated in Fig. 11. The locus of the maximum of this parable was taken for the exact time position of this impulse m. Using this technique we got an enhancement in resolution of the peak position of about a factor of 10, which results in an accuracy σ. Because the distance between the reader unit and the SAW tag is unknown or may vary and thereby the time delay to the first response impulse may be unknown or may vary too, we evaluated only the time difference between two pulses:

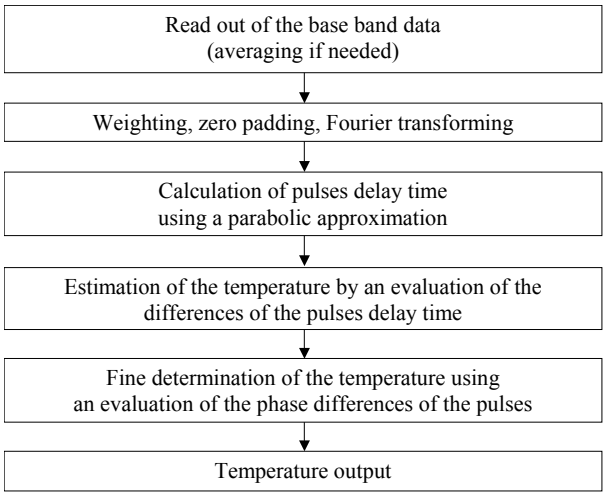

Fig. 10. Flow chart of the data analysis of a wireless passive SAW temperature sensor

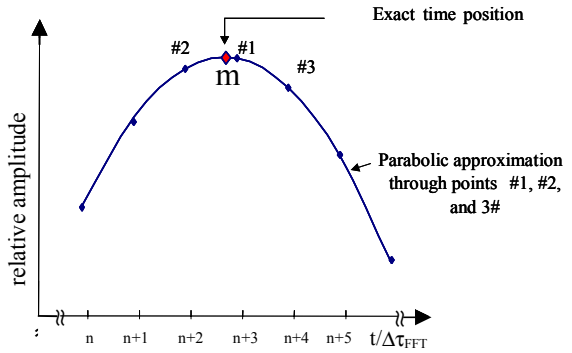

Fig. 11. Determination of the exact time position of the maximum of a pulse by using a parable approximation through the points #1, #2 and #3 around the maximum "m"

$$\tau_{2\text{-}1} = \tau_2 - \tau_1,$$

As a function of the temperature ϑ, the linear term of a Taylor series expansion usually describes the situation well enough:

$$\tau_{2-1}(\vartheta) = \tau_{2-1}(\vartheta_{ref})\left[1 + TDC_\tau \cdot (\vartheta - \vartheta_{ref})\right], \qquad (1)$$

where $TCD\tau$ is the well-known linear temperature coefficient of delay:

$$TCD_\tau = \frac{1}{\tau} \cdot \frac{\partial \tau}{\partial \vartheta}$$

Fig. 12 and 13 show the measured variation of the delay time differences $\tau_{2\text{-}1}(\vartheta)$ plus $\tau_{3\text{-}1}(\vartheta)$ between the first and second, and the first and third impulse as a function of the temperature ϑ. The gradient of the lines of best fit are with 70,8 and 70,0 ppm/°C in excellent agreement the values from literature.

In both figures a periodical variation in the delay time differences occurs, which can be affected by varying the tag position inside the oven. Therefore, these variations are more likely caused by multipath reflections inside the metallic chamber of the oven then by the signal to noise ratio of the Rx data. Fig. 14 shows the resulting inaccuracy when we try to calculate the temperature solely with the help of the delay time differences. We get an accuracy σ for the temperature of σ=10°C by evaluating $\tau_{3\text{-}1}(\vartheta)$.

The resolution can be increased significantly by evaluating the phase differences:

$$\varphi_{2-1}(\vartheta) = 2\pi\, f_0 \tau_{2-1}(\vartheta), \qquad (2)$$

Again the temperature dependence is given by:

$$\varphi_{2-1}(\vartheta) = \varphi_{2-1}(\vartheta_{ref})\left[1 + TCD_\varphi \cdot (\vartheta - \vartheta_{ref})\right], \qquad (3)$$

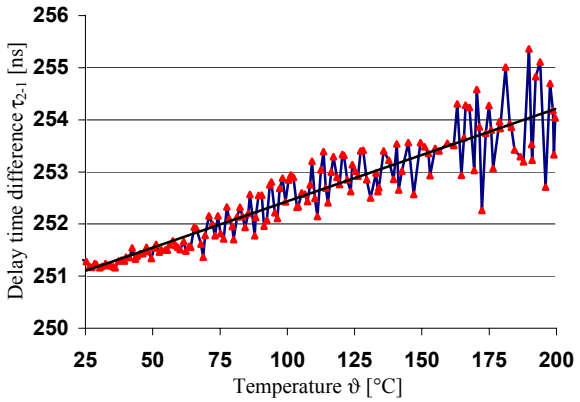

Fig. 12. Variation of the delay time difference $\tau_{2\text{-}1}(\vartheta)$ between the first and second response as a function of temperature.

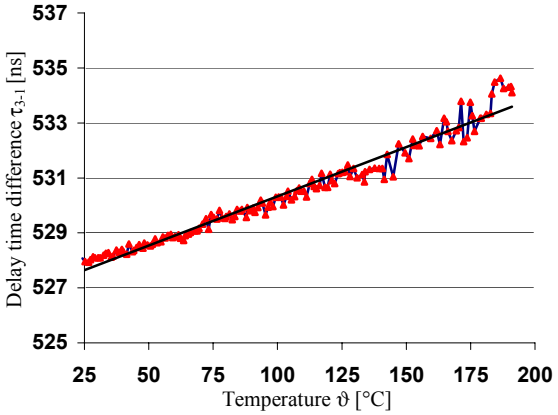

Fig. 13. Variation of the delay time difference $\tau_{3\text{-}1}(\vartheta)$ between the first and third response as a function of temperature

where TCD_φ is now the slightly different; linear temperature coefficient of phase.

The evaluation of the phase differences, however, induces an ambiguity when the phase shift exceeds 360°. Fig. 15 shows the variation of the phase difference $\varphi_{2-1}(\vartheta)$ between the first and second response as a function of temperature. We use the coarse estimation of the temperature resulting from the evaluation of $\tau_{2-1}(\vartheta)$ and $\tau_{3-1}(\vartheta)$ to overcome this equivocation of the phase evaluation. To determine the absolute phase φ_{2-1} within 2π the accuracy $\sigma_{\tau 2-1}$ of the delay time τ_{2-1} must be:

$$\frac{\sigma_{\varphi_{2-1}}}{\varphi_{2-1}} = \frac{2\pi f_0 \sigma_{\tau_{2-1}}}{2\pi f_0 \tau_{2-1}} = \frac{\sigma_{\tau_{2-1}}}{\tau_{2-1}}, \qquad (4)$$

By demanding $\sigma_{\varphi 2-1}<2\pi$, and using (2) we get:

$$\sigma_{\tau_{2-1}} < \frac{1}{f_0}, \qquad (5)$$

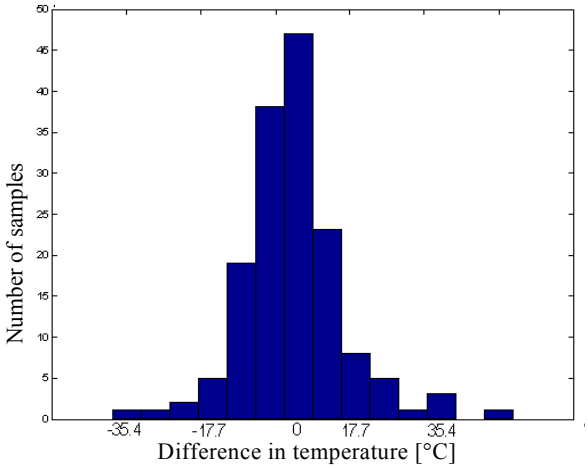

Fig. 14. Resulting error if the temperature is calculated solely by the delay time differences.

Situation becomes a little bit easier if we use a long delay time difference τ_{3-1} (with a small relative error) for the coarse estimation of the temperature and a short delay time difference τ_{2-1} (with a large unambiguousness) for the first phase evaluation. This leads to a finer determination of the temperature, which allows the phase evaluation of shorter delay time differences. The required accuracy $\sigma_{\tau 3-1}$ then becomes to:

$$\sigma_{\tau_{3-1}} < \frac{\tau_{3-1}}{\tau_{2-1}} \cdot \frac{1}{f_0}, \qquad (6)$$

The needed accuracy can be expressed in terms of the point spacing after the Fourier transformation $\Delta\tau_{FFT}$ (including the doubling of the points due to the zero padding) by:

$$\frac{\sigma_{\tau_{3-1}}}{\Delta\tau_{FFT}} < \frac{\tau_{3-1}}{\tau_{2-1}} \cdot \frac{2 \cdot B}{f_0}, \qquad (7)$$

If we assume an accuracy of:

$$\sigma_{\tau_{3-1}} = \frac{\Delta\tau_{FFT}}{5}$$

Using the parable approximation of the maximum, we get:

$$\frac{\tau_{3-1}}{\tau_{2-1}} < \frac{\sigma_{\tau_{3-1}}}{\Delta\tau_{FFT}} \cdot \frac{f_0}{2 \cdot B} \approx \frac{f_0}{10 \cdot B}, \qquad (8)$$

If we insert the data of the Baumer SAW reader system, we get a minimum ratio between the longer (τ_{3-1}) and the shorter (τ_{2-1}) delay time difference of 6. Therefore a very short delay time difference would be advantageous.

On the other hand we do need a minimum spacing to avoid intersymbol interference. Fig. 16 shows the corresponding variation of the phase difference between the pulses #5 and #4 of the RF response as a function of

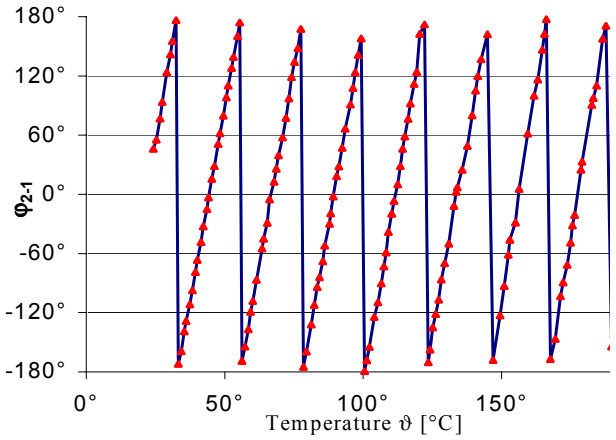

Fig. 15. Variation of the phase difference φ_{2-1} between the first and second response as a function of temperature.

temperature. The intersymbol interference between these two signals destroys the monotonic relation between temperature and phase difference. A temperature determination using this phase difference is therefore no more possible.

However, we can construct mathematically a very short delay time difference by analysing τ_{3-1}-2·τ_{2-1}. Since the delay time difference between the pulses #2 and #1 is τ_{2-1} =250 ns and between the pulses #3 and #1 is τ_{3-1} =525 ns, we get one single time slot for the weighted difference:

$$\tau_{3-1}\text{-}2\cdot\tau_{2-1} = 25 \text{ ns},$$

Fig. 17 gives the temperature characteristics of the phase at short for this very short time difference. The temperature range of unambiguousness is more than 200°C. Adding this temperature information to the coarse estimated value from the delay difference information we can eliminate one after the other ambiguity in phase differences

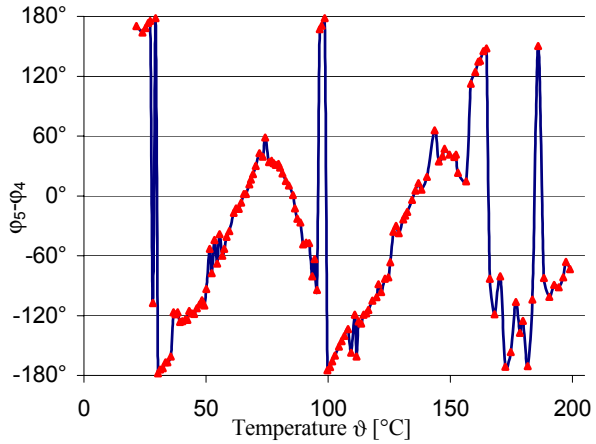

Fig. 16. Variation of the phase difference φ_{5-4} between the fifth and fourth response as a function of temperature.

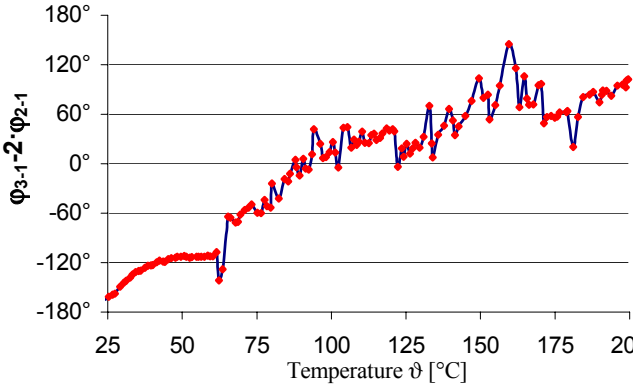

Fig. 17. Variation of the weighted difference of two phase differences $\varphi_{3-1}-2\cdot\varphi_{2-1}$ as a function of temperature.

of φ_{2-1} and φ_{3-1}. Using this technique we get the continuous phase difference φ_{3-1} between the first and third response (see Fig. 18), which allows us to determine the temperature

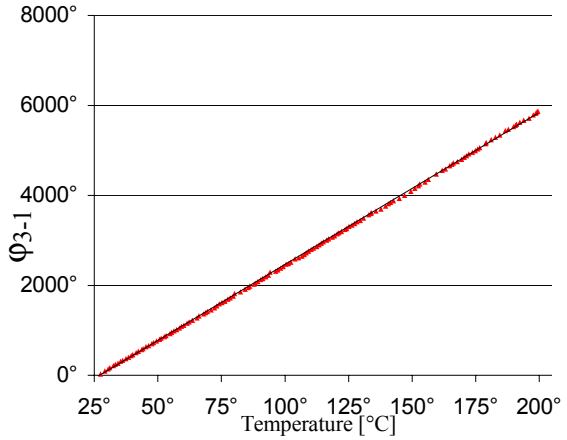

Fig. 18. Variation of the continuous phase difference φ_{3-1} between the first and third response as a function of temperature.

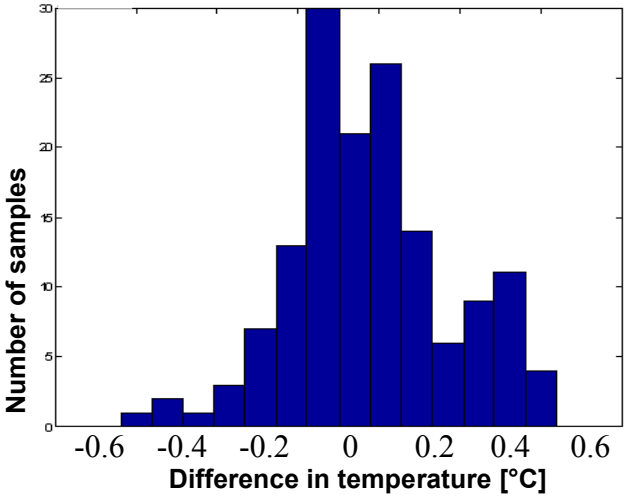

Fig. 19. Resulting error in temperature if the temperature is calculated using the continuous phase differences between the pulses #3 and #2.

with a resolution of ±0.2°C. Fig. 19 gives the resulting temperature error by using the continuous phase difference φ_{3-1}.

VI. Conclusion

By combining the principles of conventionally-wired SAW sensors with the radio-request technique, as known from SAW ID tags, a read-out of passive sensors solely by a radio-frequency link can be developed. Based on a commercially aviable read-out system developed for identification applications and the corresponding SAW transponder, we arrive at a wireless system for measuring temperature. Using a precise evaluation of the delay time differences between the responded signals we can overcome the limited temperature range of the phase evaluation. The overall measurement accuracy is in the order of ±0.2°C within a temperature range of more than 200°C. The read-out distance is up to 6 m.

References

[1] R.M. White, F.W. Voltmer, "Direct piezoelectric coupling to surface elastic waves," *Appl. Phys. Lett.*, vol. 7, pp. 314-316, 1965.

[2] P. A. Nysen, H. Skeie, D. Armstrong, "System for interrogating a passive transponder carrying phase-encoded information," *US Patents 4 725 841, 4 625 207, 4 625 208*, 1983-1986.

[3] L. Reindl, W. Ruile: "Programmable Reflectors for SAW-ID-Tags," in *Proc. of the 1993 IEEE Ultrasonics Symp.*, pp. 125-130.

[4] X. Q. Bao, W. Burkhard, V. V. Varadan, V. K. Varadan, "SAW Temperature Sensor and Remote Reading System," in *Proc. of the 1987 IEEE Ultrasonics Symp.*, pp. 583-585.

[5] L. Reindl, G. Scholl, T. Ostertag, H. Scherr, U. Wolff, F. Schmidt, "Theory and application of passive SAW radio transponders as sensors," *IEEE Transactions on UFFC,* vol. 45, No. 5, Sep. 1998, pp. 1281-1292.

[6] L. Reindl, A. Pohl, G. Scholl, R. Weigel, "SAW-Based Radio Sensor Systems" IEEE Sensors Journal, vol. 1, No. 1 , Jun 2001, pp. 69 –78.

[7] M. I. Skolnik, "Introduction to Radar Systems," New York etc.: McGraw Hill, 1979.

[8] R. Peter and C.S. Hartmann, "Passive long range and high temperature ID systems based on SAW technology,", Sensor 2003, Nürnberg, May 2003.

[9] A. Steindl, A. Pohl, L. Reindl, J. Hornsteiner, E. Riha, F. Seifert, "Passive Surface Acoustic Waves Sensors for Temperature and Other Measurands," Tempmeko Proceedings, 1999.

[10] M. Kunz, S. Schlatter. "Passive, Contactless Temperature Sensor," Second term paper, Hochschule Rapperswil. Switzerland, 1999.